International Journal of Nanomedicine

Dovepress
Taylor & Francis Group

Open Access Full Text Article

ORIGINAL RESEARCH

Vancomycin-Loaded Isogenous Membrane Vesicles for Macrophage Activation and Intracellular Methicillin-Resistant *Staphylococcus aureus* Elimination

Jianxiong Dou[1,*], Weilong Shang[1,*], Huagang Peng[1], Yi Yang[1], Juan Chen[2], Yifan Rao[3], Li Tan[1], Zhen Hu[1], Yuting Wang[1], Xiaonan Huang[1], Yuhua Yang[1], Jianghong Wu[1], Qiwen Hu[1], Chuan Xiao[1], Xiancai Rao[1,3]

[1]Department of Microbiology, College of Basic Medical Sciences, Army Medical University, Key Laboratory of Microbial Engineering Under the Educational Committee in Chongqing, Chongqing, 400038, People's Republic of China; [2]Department of Pharmacy, Xinqiao Hospital, Army Medical University, Chongqing, 400037, People's Republic of China; [3]Department of Emergency Medicine, Xinqiao Hospital, Army Medical University, Chongqing, 400037, People's Republic of China

*These authors contributed equally to this work

Correspondence: Xiancai Rao; Chuan Xiao, Email xcrao@tmmu.edu.cn, raoxiancai@126.com; xiaochuanapple@tmmu.edu.cn

Introduction: Methicillin-resistant *Staphylococcus aureus* (MRSA), a notorious multidrug-resistant (MDR) pathogen, frequently resides and proliferates within macrophages, contributing to refractory and recurrent infections. Conventional antibiotics exhibit limited efficacy against intracellular MRSA due to poor cellular penetration.

Methods: Vancomycin (VAN) was encapsulated into membrane vesicles ($^{\Delta agrA}$MVs) derived from the attenuated *S. aureus* strain RN4220Δ*agrA*, generating VAN-loaded nanoparticles ($^{\Delta agrA}$MV-VAN). In vitro and in vivo experiments were performed to test the efficacy of $^{\Delta agrA}$MV-VAN in intracellular MRSA clearance.

Results: $^{\Delta agrA}$MV-VAN demonstrated sustained VAN release and efficient extracellular MRSA eradication. Moreover, macrophages actively internalized $^{\Delta agrA}$MV-VAN, leading to VAN accumulation in intracellular compartments and M1 macrophage polarization, which increased MRSA killing. In vivo animal experiments revealed that $^{\Delta agrA}$MV-VAN was safe and effectively eliminated intracellular MRSA in abdominal infections.

Conclusion: Our findings propose a nanotherapeutic strategy that uses bacterial-derived vesicles for targeted antibiotic delivery, overcoming the intrinsic limitations of conventional therapies against intracellular MDR pathogens.

Keywords: MRSA, $^{\Delta agrA}$MV-VAN nanoparticles, macrophage activation, intracellular infections, intracellularly bacterial clearance

Introduction

Infectious diseases caused by bacteria, particularly multidrug-resistant (MDR) strains, pose a serious threat to human health.[1] Methicillin-resistant *Staphylococcus aureus* (MRSA) is a prominent MDR pathogen known for its rapid spread and ability to cause various infections, ranging from common wound infections to lethal pneumonia, osteomyelitis, and sepsis.[2] The resistance of MRSA to multiple clinically relevant drugs, such as methicillin, erythromycin, and clindamycin, complicates treatment and control efforts.[3] Structure-based virtual screening has identified potential inhibitors targeting key *S. aureus* determinants, including the glycopeptide-resistance regulator GraR,[4] methicillin-resistance-associated FmtA,[5] GTPase YsxC,[6] and lipophilic membrane,[7] which may serve as leads for novel anti-MRSA agents. Notably, MRSA can subvert the innate immune system of macrophages and proliferate intracellularly, promoting chronic and recurrent infections.[8,9] Vancomycin (VAN) is considered as a last-resort drug for severe MRSA infections.[10]

Received: 22 February 2025
Accepted: 7 June 2025
Published: 17 June 2025

Graphical Abstract

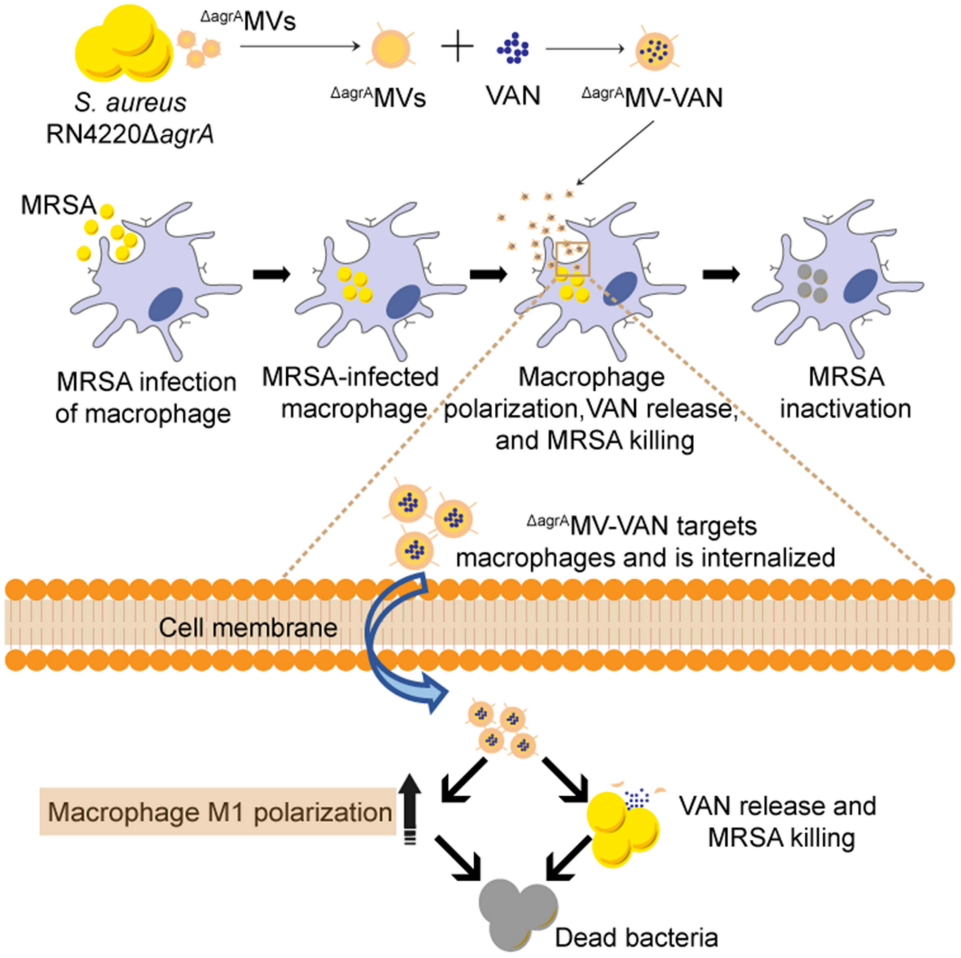

However, the poor cellular penetration and rapid macrophage clearance of VAN limit its efficacy against intracellular pathogens.[9,11,12] Therefore, enhancing drug delivery to achieve high intracellular accumulation represents a promising strategy for eradicating persistent MRSA infections.

Nanodrug carriers substantially improve transmembrane permeability, intracellular accumulation, and antimicrobial activity of encapsulated drugs against intracellular infections caused by MDR pathogens.[13,14] A variety of nanodrug carriers, such as liposomes,[15] poly(lactic-co-glycolic acid) particles,[16] exosomes,[17] and inorganic nanoparticles,[18] have been developed to enhance drug delivery efficiency to macrophages. Among these, bacterial membrane vesicles (MVs), lipid-bound nanoparticles (20–400 nm in diameter) spontaneously released during bacterial growth, have emerged as attractive nanodrug carriers.[19,20] These MVs are enriched with proteins, peptidoglycans, DNA, and RNA, most of which are pathogen-associated molecular patterns (PAMPs) capable of targeting and activating immune cells, including macrophages, to kill intracellular pathogens.[19] While MVs derived from Gram-negative bacteria such as *Escherichia coli* have been widely explored for antibiotic delivery,[18] they frequently contain lipopolysaccharide (LPS), a membrane–bound endotoxin that contributes to bacterial pathogenicity.[20] In contrast, Gram-positive bacteria such as *S. aureus* produce LPS-free MVs with superior biocompatibility.[20] Additionally, *S. aureus* MVs demonstrate high macrophage uptake efficiency.[21] Notably, multiple studies have revealed that MVs are favorably internalized by their homologous bacteria,[22–24] implying an intrinsic targeting capability of bacterial MVs.

In our previous study, we constructed an attenuated *S. aureus* strain, RN4220Δ*agrA*, and demonstrated the hypotoxicity of $^{\Delta agrA}$MVs to macrophages.[25] Herein, we hypothesized that isogenic $^{\Delta agrA}$MVs encapsulated with VAN would be favorably targeted and taken up by MRSA-infected macrophages, enhancing intracellular bacterial killing. To evaluate the nanodrug carrier potential of *S. aureus* MVs, we prepared VAN-loaded $^{\Delta agrA}$MVs ($^{\Delta agrA}$MV-VAN). These nanoparticles exhibited a sustained-release profile and were sufficiently internalized by macrophages. Moreover, $^{\Delta agrA}$MV treatment promoted macrophage polarization toward the M1 phenotype, which facilitated the clearance of intracellular MRSA. $^{\Delta agrA}$MV-VAN demonstrated excellent safety, and treatment with $^{\Delta agrA}$MV-VAN effectively killed MRSA in macrophages in both in vitro and in vivo models. Collectively, this study provides a new design for isogenic nanomedicines that combines efficient drug delivery with potent antimicrobial activity against intracellular infections.

Materials and Methods

Bacterial Strains and Culture

The *S. aureus* strain RN4220Δ*agrA* was generated previously,[25] and the strain USA300 (FPR3757) was kindly provided by Dr. Min Li (Shanghai Jiao Tong University, China). *S. aureus* strains were cultured in brain heart infusion (BHI) medium (Oxoid, UK) or on BHI agar (BHIA) at 37 °C.

Preparation of $^{\Delta agrA}$MVs and $^{\Delta agrA}$MV-VAN

$^{\Delta agrA}$MVs were prepared from the culture supernatant of *S. aureus* strain RN4220Δ*agrA* as previously described.[23,25] Briefly, a single colony of RN4220Δ*agrA* grown on BHIA was picked, inoculated into fresh BHI broth, and cultivated at 37 °C for 12 h with agitation. Subsequently, the culture was diluted 1:100 in 300 mL of fresh BHI broth and incubated at 37 °C for another 12 h. The supernatant containing $^{\Delta agrA}$MVs was collected by centrifugation at 6000 ×g for 10 min, followed by centrifugation at 10,000 ×g for 10 min, and filtered through a 0.22 μm membrane filter (Merck Millipore, USA) to remove dead cells and cellular debris. The resulting solution was concentrated by ultrafiltration using a 100 kDa hollow fiber membrane column (GE Healthcare, USA) to enrich $^{\Delta agrA}$MVs. After ultracentrifugation at 200,000 ×g with a rotor (HITACHI, Japan) for 3 h, the $^{\Delta agrA}$MV pellets were resuspended in 4 mL of 50% (v/v) Optiprep density gradient solution (Alere Technologies AS, Norway), followed by sequential layering with 2 mL of 40% Optiprep, 2 mL of 20% Optiprep, and 1.5 mL of 10% Optiprep. After centrifugation at 200,000 ×g for 3 h at 4°C, the solution was divided into five fractions from top to bottom, transferred into sterile tubes, and analyzed by SDS-PAGE (Servicebio, China). The $^{\Delta agrA}$MVs located between the 20% and 40% Optiprep layers were carefully extracted, concentrated using an ultrafiltration tube (Millipore), resuspended in phosphate-buffered saline (PBS), and stored at −80 °C until use.

VAN-loaded $^{\Delta agrA}$MVs ($^{\Delta agrA}$MV-VAN) were prepared as previously described.[26] In brief, VAN (Sigma-Aldrich, USA) and $^{\Delta agrA}$MVs were mixed at mass ratios of 1:1, 1:2, or 2:1 and subjected to sonication using a UP-50H Ultrasonic cell disruptor (Hielscher, Germany) at 30% power for six cycles (4 s pulse, 2 s pause). The mixture was then incubated at 37 °C for 1 h to allow $^{\Delta agrA}$MVs reformation. Free VAN was removed by ultrafiltration using an Amicon® Ultracentrifugal filter (MWCO = 100 kDa, GE Healthcare, UK). The purified $^{\Delta agrA}$MV-VAN was aseptically filtered through a 0.22 μm syringe filter (Millipore) and stored at −80°C.

Characterization of $^{\Delta agrA}$MVs and $^{\Delta agrA}$MV-VAN

$^{\Delta agrA}$MV samples were dropped onto copper grids, allowed to sediment naturally for15 min,negatively stained with 2% (v/v) phosphotungstic acid for 15 s, and air-dried for 1 h.[20] The morphology of $^{\Delta agrA}$MVs and $^{\Delta agrA}$MV-VAN was observed using transmission electron microscopy (TEM; HT7700, Hitachi, Japan). The particle size distribution and zeta potential of $^{\Delta agrA}$MVs and $^{\Delta agrA}$MV-VAN were measured by dynamic light scattering (DLS) using a Nanoparticle Size Analyzer (Zatasizer Nano ZSP, Malvern, USA).

VAN Release

High-performance liquid chromatography (HPLC) was performed to quantify $^{\Delta agrA}$MV-VAN as previously reported.[26] Briefly, freshly prepared $^{\Delta agrA}$MV-VAN was enclosed in a dialysis bag (MWCO:100 kDa; Ruiswbio, USA) and incubated

at 37 °C with shaking. At each time point, 1 mL aliquots were collected and analyzed by HPLC. Each aliquot was mixed with an appropriate volume of acetonitrile in a centrifuge tube. After sonication, the supernatant was collected by centrifugation at 18,000 ×g for 10 min, filtered through a 0.22 μm syringe filter, and transferred to an HPLC auto-sampler. Approximately 1 mL of the sample was injected into the HPLC system (Agilent 1260, Agilent Technologies, CA) equipped with a C18 column (extended-C18, 250 mm × 4.6 mm, 5 μm, 100 Å, Agilent). The mobile phase (KH_2PO_4 :acetonitrile, 90.5: 9.5, v/v, pH = 3.2) was used at 30 °C with a flow rate of 1 mL/min. VAN elution was monitored at 236 nm, and a standard curve was established using VAN concentrations ranging from 3.125 to 50 μg/mL with OpenLAB CDS ChemStation Edition software. The release profile of VAN from $^{\Delta agrA}$MV-VAN was evaluated in PBS (pH 7.4).

Direct Killing of MRSA by $^{\Delta agrA}$MV-VAN

The bactericidal activity of $^{\Delta agrA}$MV-VAN against planktonic MRSA was determined as previously described.[27] Briefly, overnight cultured MRSA USA300 was diluted with PBS to 1×10^6 colony-forming units per milliliter (CFU/mL), and 100 μL of the bacterial suspension was added to each well of a 96-well plate. Next, 100 μL of PBS, VAN (5 μg/mL), $^{\Delta agrA}$MVs (25 μg/mL), $^{\Delta agrA}$MVs (25 μg/mL) plus VAN (5 μg/mL), or $^{\Delta agrA}$MV-VAN (25 μg/mL) was added to each well. Afterward, the plates were incubated at 37 °C for 24 h. At 0, 2, 6, 12, and 24 h post-incubation, 10 μL aliquots were collected from each well for CFU enumeration. After 24 h of treatment, bacterial cells were collected and stained using a LIVE/DEAD BacLight Bacterial Viability kit (APExBIO, USA). Cell viability was assessed using confocal laser scanning microscopy (LSM880, Zeiss, Germany).

In vitro Cellular Uptake of $^{\Delta agrA}$MVs and $^{\Delta agrA}$MV-FITC-VAN

Mouse RAW264.7 macrophages (HaiStar Biotech, Beijing, China; Cat. No. TCM-C766) were cultured in Dulbecco's Modified Eagle Medium (DMEM; Zeta Life, USA) supplemented with 10% fetal bovine serum (FBS; Thermo Fisher Scientific, USA) and 1% (v/v) penicillin-streptomycin solution (Zeta Life, USA) at 37 °C with 5% (v/v) CO_2. For cell uptake experiments, RAW264.7 cells (1×10^5 cells/well) were seeded in confocal dishes (In Vitro Scientific, China) and incubated overnight at 37 °C. $^{\Delta agrA}$MVs, liposomes (Abnova, China), and $^{\Delta agrA}$MVs pretreated with proteinase K (2 μg/mL; Beyotime, China) were labeled with 30 μM DiO dye (Dalian Meilun Biotech, China) at 37 °C for 90 min. Cells were then treated with DiO-labeled $^{\Delta agrA}$MVs, liposomes, or proteinase K-treated $^{\Delta agrA}$MVs (PK; 5 μg per dish). After 90 min of incubation at 37 °C with 5% (v/v) CO_2, the culture medium was removed, and cells were washed twice with PBS. Cells were fixed with 500 μL of 4% paraformaldehyde (Biosharp, China) at room temperature for 15 min, followed by nuclear staining with 200 μL of 4',6-diamidino-2-phenylindole (DAPI; Dowobio, China) for 10 min. After washing twice with PBS (4 min each), cells were observed under a super-resolution laser scanning confocal microscope (LSM880, Zeiss, Germany). DiO (green fluorescence) and DAPI exhibited maximum excitation wavelengths of 484 nm and 358 nm, respectively.

FITC-labeled VAN (FITC-VAN; Ruixibio, Xi'an, China) was used to prepare $^{\Delta agrA}$MV-FITC-VAN formulation at a 1:2 mass ratio. For uptake experiment, RAW264.7 macrophages were treated with either FITC-VAN (3 μg/dish) or $^{\Delta agrA}$MV-FITC-VAN (15 μg/dish). Fluorescence intensity was detected by confocal laser scanning microscopy (CLSM).[20]

Inflammatory Factor Detection

RAW264.7 macrophages were seeded in 24-well plates at a density of 1×10^5 cells/well and incubated overnight at 37 °C with 5% (v/v) CO_2. The following day, cells were treated with VAN (5 μg/mL), liposomes (5 μg/mL), or $^{\Delta agrA}$MVs (5 μg/mL). An equal volume of PBS was used as a negative control. After 12 h of treatment, culture supernatants were collected, and the levels of inflammatory factors TNF-α and IL-6 were detected using an enzyme-linked immunosorbent assay (ELISA) kit (MEIMIAN, China).[20]

Macrophage Polarization Analysis

RAW264.7 macrophages cultured in confocal dishes were treated with $^{\Delta agrA}$MVs (5 μg/mL) for 12 or 24 h. Untreated cells were used as blank controls, while PBS-treated cells served as negative controls. After fixation with 4% (v/v)

paraformaldehyde, macrophage polarization was assessed using anti-mouse CD86 antibodies (Multisciences, China). $CD86^+$ cells, representing M1-polarized macrophages, were analyzed by flow cytometry (Challenbio, China) and CLSM (LSM880) as described.[28,29]

MRSA Killing by $^{\Delta agrA}$MV-Activated Macrophages

Methicillin-resistant *S. aureus* (MRSA) infection was performed as previously described.[30] For assessing $^{\Delta agrA}$MV-mediated macrophage killing of MRSA, RAW264.7 cells were seeded in 24-well plates (1×10^5 cells/well) and cultured overnight at 37 °C with 5% CO_2. Cells were then infected with MRSA USA300 at a multiplicity of infection (MOI) of 15 (approximately 5×10^6 CFU/well). After 2 h of infection, extracellular bacteria were eliminated by treatment with 20 μg/mL lysostaphin (Sigma-Aldrich, USA) for 20 min. Afterward, fresh DMEM medium supplemented with VAN (2.5 μg/mL), liposomes (2.5 μg/mL), or $^{\Delta agrA}$MVs (2.5 μg/mL) was added, followed by incubation for an additional 12 h. PBS was used as a negative control. Intracellular bacterial counts were determined by plate assay.[18] In brief, infected cells were collected by centrifugation at 6000 ×g for 10 min at 4 °C. Cell pellets were treated with 15 μg/mL lysostaphin for 20 min at room temperature, washed thrice with PBS, and lysed with Hank's Balanced Salt Solution (Servicebio, China) containing 0.2% (v/v) Triton X-100 for 10 min. Subsequently, intracellular CFUs were quantified using BHI agar plate dilution assays.

For evaluating $^{\Delta agrA}$MV-activated macrophage killing of MRSA, RAW264.7 cells were pretreated for 2 h with VAN, liposomes, or $^{\Delta agrA}$MVs at various concentrations (0, 2.5, 5.0, and 10.0 μg/mL). Following treatment, MRSA infection was conducted as above. After lysostaphin treatment (20 μg/mL) to eliminate extracellular bacteria and replacement with fresh DMEM, intracellular MRSA counts were detected 12 and 24 h post-infection.

Intracellular MRSA Killing by $^{\Delta agrA}$MV-VAN

RAW264.7 cells were cultured in 24-well plates and infected with MRSA USA300 at an MOI of 20 as described above. The infected cells were then cultured in fresh DMEM supplemented with $^{\Delta agrA}$MV-VAN (25 μg/mL). Control groups included MRSA-infected cells treated with PBS, VAN alone (5 μg/mL), $^{\Delta agrA}$MVs alone (25 μg/mL), and $^{\Delta agrA}$MV (25 μg/mL) + VAN (5 μg/mL). Intracellular bacterial loads were counted at 12 and 24 h post-infection.

In vivo Anti-MRSA Effect of $^{\Delta agrA}$MV-VAN

Female BALB/c mice (6–8 weeks old) were obtained from Chongqing Byrness Weil Biotechnology Co., Ltd. (Chongqing, China). All animal experiments were approved by the Laboratory Animal Welfare and Ethics Committee of Army Medical University (Approval No. AMUWEC2020735).

A murine abdominal infection model was established as previously described.[18] Briefly, 20 BALB/c mice were intraperitoneally inoculated with 5×10^7 CFU of MRSA USA300 and randomly allocated into five groups: (1) PBS (negative control), (2) VAN (10 mg/kg; positive control), (3) $^{\Delta agrA}$MVs (6 mg/kg), (4) $^{\Delta agrA}$MV+VAN (equivalent individual doses), and (5) $^{\Delta agrA}$MV-VAN (6 mg/kg). After 24 h of treatment, mice were anesthetized with 1% (w/v) pentobarbital sodium, followed by peritoneal lavage with 3 mL sterile PBS. All animals were euthanized on day 2 post-infection. Peritoneal lavage fluid was centrifuged at 6000 ×g for 10 min at 4 °C to pellet cells. Bacterial loads in both the supernatant (extracellular) and cell lysates (intracellular) were counted separately.

Safety Assessment

RAW264.7 cells were used to assess the cytotoxicity of $^{\Delta agrA}$MV-VAN using the 3-[4,5-dimethylthiazol-2-yl]-2,5-diphenyltetrazolium bromide (MTT) assay as previously described.[18] In brief, RAW264.7 macrophages were seeded in 96-well plates (2×10^3 cells/well) and cultured for 24 h at 37 °C with 5% (v/v) CO_2. The culture medium was replaced with fresh medium supplemented with different concentrations of $^{\Delta agrA}$MVs (0, 25, 50, 100, and 200 μg/mL). Cell viability was detected 2, 6, 12, and 24 h after treatment using a Cell Counting Kit (Zeta Life).

A mouse abdominal infection model was generated (n = 3 per group) and treated with PBS, VAN (10 mg/kg), $^{\Delta agrA}$MVs (6 mg/kg), or $^{\Delta agrA}$MV-VAN (6 mg/kg). After 24 h of treatment, MRSA-infected mice were sacrificed, and organs (including the heart, liver, spleen, lungs, and kidneys) were harvested and fixed with 4% (v/v) paraformaldehyde.

Histopathological examination was then performed on organ sections using hematoxylin and eosin (H&E) staining. Serum IL-6 and TNF-α levels at 6 h post-treatment were determined using an ELISA kit (MEIMIAN).

Statistical Analysis

All experiments were repeated at least three times, and the data are expressed as the mean ± standard deviation (SD) or standard error of the mean (SEM). Statistical comparisons were performed using GraphPad Prism 9.5 program (GraphPad Software, USA). The significance of differences between groups was assessed using Student's *t*-test, one-way analysis of variance (ANOVA), or two-way ANOVA. A *P*-value of < 0.05 was considered statistically significant.

Results and Discussion

Preparation and Characterization of $^{\Delta agrA}$MVs and $^{\Delta agrA}$MV-VAN Particles

The quorum-sensing accessory gene regulator (*agr*) is a major factor that controls *S. aureus* virulence.[31,32] We previously showed that *agr* deletion remarkably decreased the virulence of MVs in *S. aureus* strain RN4220.[20] Therefore, we used the engineered RN4220Δ*agrA* as the starting strain.[25] $^{\Delta agrA}$MVs were prepared from the culture supernatant of RN4220Δ*agrA*. After density gradient centrifugation, the $^{\Delta agrA}$MVs was verified by SDS-PAGE, and were found to be mainly located between 20% and 40% Optiprep (Figure S1). TEM analysis exhibited the nanoscale vesicles of $^{\Delta agrA}$MVs (Figure 1a). The protein concentration of $^{\Delta agrA}$MVs was determined (Figure S2), and VAN-loaded $^{\Delta agrA}$MVs were prepared using an ultrasonic method as previously described.[18] VAN-loaded liposomal formulations often have low encapsulation efficiencies, ranging from 0.1% to 9%.[11] To achieve high drug-loading efficiency, $^{\Delta agrA}$MVs:VAN mass ratios of 1:1, 1:2, and 2:1 were used. The results indicated that the $^{\Delta agrA}$MVs:VAN ratio of 1:2 achieved the highest VAN loading ratio of 21.6%, which was significantly higher than those at 1:1 (6.3%) and 2:1 (2.0%; $P < 0.001$; Figure 1b). TEM observations demonstrated that $^{\Delta agrA}$MV-VAN maintained its spherical shape (Figure 1c). DLS measurements

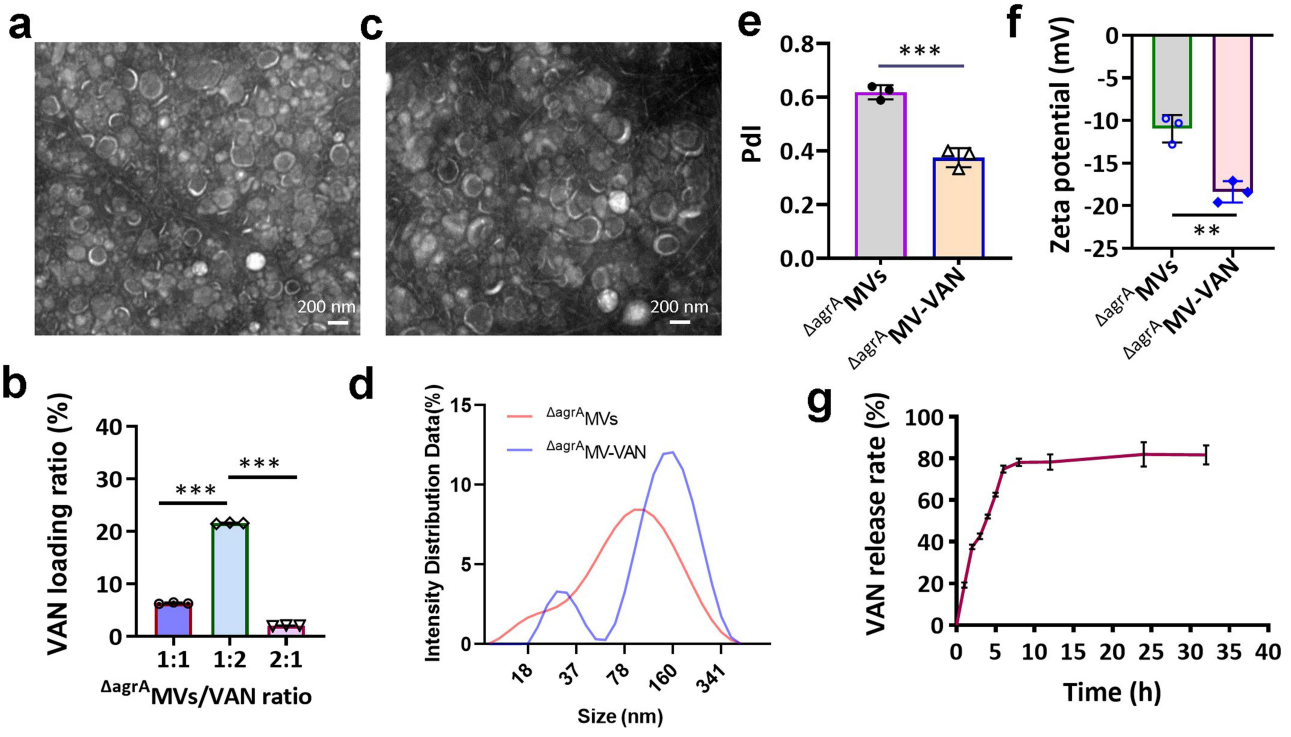

Figure 1 Characterization of $^{\Delta agrA}$MVs and $^{\Delta agrA}$MV-VAN. (**a**) Transmission electron microscopy (TEM) image showing the spherical morphology of $^{\Delta agrA}$MVs (scale bar: 200 nm). (**b**) VAN loading efficiency with various $^{\Delta agrA}$MVs:VAN mass ratios. (**c**) TEM image of $^{\Delta agrA}$MV-VAN nanoparticles. (**d**) Particle size distribution of $^{\Delta agrA}$MVs and $^{\Delta agrA}$MV-VAN detected by dynamic light scattering (DLS). (**e**) PDI values of $^{\Delta agrA}$MVs and $^{\Delta agrA}$MV-VAN detected by DLS. (**f**) Zeta potential of $^{\Delta agrA}$MVs and $^{\Delta agrA}$MV-VAN measured by DLS. (**g**) In vitro VAN release profile from $^{\Delta agrA}$MV-VAN in neutral PBS, quantified by HPLC. Data are shown as mean ± SD ($n = 3$). Statistical significance was calculated by Student's *t*-test, ** $P < 0.01$, and *** $P < 0.001$.

indicated that the mean size of $^{\Delta agrA}$MVs was 71 nm, whereas the particle size of $^{\Delta agrA}$MV-VAN increased to 101 nm (Figure 1d). Xie et al[18] found that the size of VAN-loaded and polydopamine-encapsulated mesoporous SiO_2 nanoparticles increased from 106 to 122 nm after coating with *E. coli* MVs. This phenomenon indicated the versatile potential of bacterial MVs as drug carriers.

Polydispersity index (PDI) determination revealed that $^{\Delta agrA}$MV-VAN had a decreased PDI from 0.6 ($^{\Delta agrA}$MVs) to 0.38 (Figure 1e), along with an increase in the absolute value of the membrane surface potential (Figure 1f). These data indicate that the uniformity of $^{\Delta agrA}$MV particles improved after loading VAN under our experimental conditions. HPLC was performed to determine the VAN content in $^{\Delta agrA}$MV-VAN according to a standard curve (Figure S3). The results showed that approximately 80% of the VAN was released from $^{\Delta agrA}$MV-VAN within 8 h under neutral conditions (Figure 1g). Overall, the prepared $^{\Delta agrA}$MV-VAN maintained a spherical, nanosized shape with relative homogeneity compared to $^{\Delta agrA}$MVs, and the VAN-loaded $^{\Delta agrA}$MV particles exhibited a sustained release effect.

MRSA Killing Effect of $^{\Delta agrA}$MV-VAN In Vitro

To address the resistance of *S. aureus*, many structure-based virtual screening methods have been developed to target antibiotic-resistance-associated determinants such as GraR and FmtA.[4,5] The screened compounds or inhibitors are potential antimicrobial agents against MRSA after molecular dynamics, pharmacophore modeling, and binding free energy analyses.[4–7] However, the application of these identified molecules against MRSA infections can only be realized after further experimental evaluation. To assess the anti-staphylococcal effect of $^{\Delta agrA}$MV-VAN, agar plate counting was performed as previously described.[10] As shown in Figure 2a, the minimal inhibitory concentration (MIC) of $^{\Delta agrA}$MV-VAN against MRSA USA300 was 12.5 μg/mL. Approximately 1×10^6 CFUs of *S. aureus* USA300 cells were treated with 10 μg/mL VAN, 50 μg/mL $^{\Delta agrA}$MVs, $^{\Delta agrA}$MV+VAN (10 μg/mL VAN + 50 μg/mL $^{\Delta agrA}$MVs), or 50 μg/mL $^{\Delta agrA}$MV-VAN. Plate counting was conducted at 0, 2, 6, 12, and 24 h post-culture, and the results indicated that $^{\Delta agrA}$MVs exhibited no bacteriostatic activity, showing bacterial counts similar to those of the PBS control (Figure 2b). However, the VAN-loaded $^{\Delta agrA}$MV formulation ($^{\Delta agrA}$MV-VAN) showed antimicrobial activity comparable to that of the free VAN and the $^{\Delta agrA}$MV+VAN combination, except at the 6-h time point, where the $^{\Delta agrA}$MV-VAN treatment group showed a slightly higher survival rate than the free VAN and $^{\Delta agrA}$MV+VAN groups (Figure 2c). We hypothesized that the slow-release effect of $^{\Delta agrA}$MV-VAN might account for this phenomenon. Notably, complete elimination of MRSA USA300 at 12 h post-incubation was achieved in the VAN, $^{\Delta agrA}$MV+VAN, and $^{\Delta agrA}$MV-VAN groups (Figure 2b and c).

CLSM, equipped with a LIVE/DEAD cell staining kit, allowed direct visualization of bacterial inactivation, where live bacteria (labeled with calcein-AM) appeared green, and dead cells (stained with propidium iodide, PI) appeared red.[33] As shown in Figure 2d, treatment with VAN, $^{\Delta agrA}$MV+VAN, and $^{\Delta agrA}$MV-VAN considerably increased red fluorescence (dead cells) compared to the PBS and $^{\Delta agrA}$MV groups. This finding was consistent with the plate counting results (Figure 2b), indicating that the encapsulation of VAN in *S. aureus* $^{\Delta agrA}$MVs did not compromise the antibacterial activity of VAN.

Cellular Uptake of $^{\Delta agrA}$MV Nanoparticle by Macrophages in vitro

Studies have shown that MVs derived from *S. aureus* can be efficiently taken up by macrophages, a process mediated by motor proteins on the MV surface.[33] While primary macrophages derived from human peripheral blood mononuclear cells may offer greater physiological relevance for modeling intracellular infections,[34] stable macrophage cell lines such as human THP-1 and murine RAW264.7 have been widely utilized in developing intracellular infection models.[35–37] To evaluate the potential of $^{\Delta agrA}$MVs as a vehicle for intracellular drug delivery, we used the RAW264.7 cell line to assess the uptake efficiency of $^{\Delta agrA}$MVs by macrophages. Commercial liposomes, which are established drug delivery carriers,[15] served as controls. DiO-labeled $^{\Delta agrA}$MVs or liposomes were co-incubated with RAW264.7 cells, and the green fluorescence intensity within macrophages was visualized using CLSM (Figure 3a). The fluorescence intensity was significantly higher in the $^{\Delta agrA}$MV group than in the liposome group ($P < 0.01$; Figure 3b). However, uptake was inhibited when $^{\Delta agrA}$MVs were pretreated with proteinase K (PK) for 1 h ($^{\Delta agrA}$MVs (PK)), suggesting that this phenomenon may be attributed to the degradation of surface-associated proteins on $^{\Delta agrA}$MVs.[33]

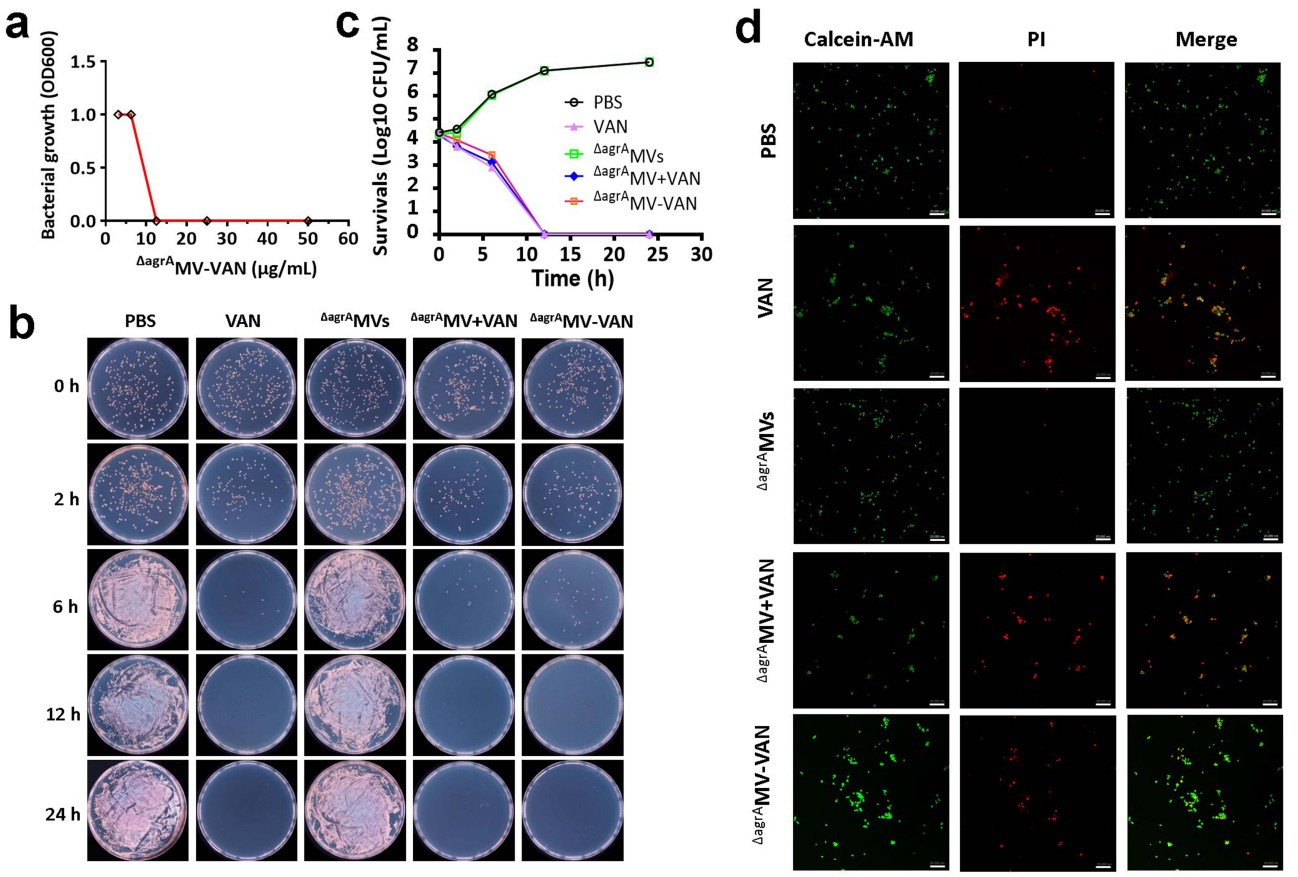

Figure 2 In vitro antibacterial activity of $^{\Delta agrA}$MV-VAN. (**a**) Minimum inhibitory concentration (MIC) of $^{\Delta agrA}$MV-VAN against MRSA USA300. (**b**) Growth inhibition of MRSA USA300 by $^{\Delta agrA}$MV-VAN. Approximately 1×10^6 CFU of bacteria were treated with 50 μg/mL $^{\Delta agrA}$MV-VAN for diverse times as indicated, and the grown bacteria on agar plates were shown. The treatment of PBS, free VAN (10 μg/mL), $^{\Delta agrA}$MVs (50 μg/mL), or $^{\Delta agrA}$MV+VAN combination (10 μg/mL VAN + 50 μg/mL $^{\Delta agrA}$MVs) served as controls. (**c**) The time-killing kinetics of $^{\Delta agrA}$MV-VAN against MRSA USA300. (**d**) CLSM images of MRSA USA300 after 24 h treatment with $^{\Delta agrA}$MV-VAN, stained with LIVE/DEAD BacLight Bacterial Viability Kit. Green fluorescence represents live bacteria, while red one indicates dead cells. Scale bars: 20 μm.

To determine whether VAN loading affected $^{\Delta agrA}$MV uptake efficiency, we examined the internalization of $^{\Delta agrA}$MV-VAN nanoparticles by RAW264.7 cells. Fluorescein isothiocyanate (FITC)-labeled VAN (FITC-VAN) was used to generate the nanomaterial $^{\Delta agrA}$MV-FITC-VAN. CLSM revealed that the uptake of $^{\Delta agrA}$MV-FITC-VAN by RAW264.7 macrophages was remarkably enhanced compared to free FITC-VAN (Figure 3c). Quantitative fluorescence analysis confirmed that the $^{\Delta agrA}$MV-FITC-VAN formulation significantly improved VAN uptake efficiency ($P < 0.001$; Figure 3d). Overall, these results indicate that $^{\Delta agrA}$MV-VAN can efficiently deliver VAN to macrophages. Given that high intracellular drug concentrations are crucial for killing intracellular pathogens,[12] the enhanced internalization of VAN mediated by $^{\Delta agrA}$MVs may facilitate the clearance of intracellular MRSA within macrophages.

Effect of $^{\Delta agrA}$MVs on Macrophage Polarization

Macrophages exhibit two activation phenotypes in response to external stimuli: M1 and M2, which are closely associated with inflammatory responses.[28,38] M2 macrophages characterized by an altered metabolic state or impaired bactericidal activity, can provide a niche for the long-term survival of intracellular bacteria, contributing to persistent and recurrent infections.[3,39] The MVs secreted by bacteria contain diverse biomolecules, such as proteins, lipids, nucleic acids, and metabolites, which play crucial roles in bacterial physiology like resistance transfer.[19,40] Studies have shown that bacterial MVs containing various PAMPs can modulate macrophage activation.[41–43] To determine the effect of *S. aureus* RN4220Δ*agrA*-derived $^{\Delta agrA}$MVs on macrophage activation, we treated RAW264.7 cells with $^{\Delta agrA}$MVs for 12 h. As shown in Figure 4a and b, $^{\Delta agrA}$MV treatment considerably increased TNF-α and IL-6 levels compared to the

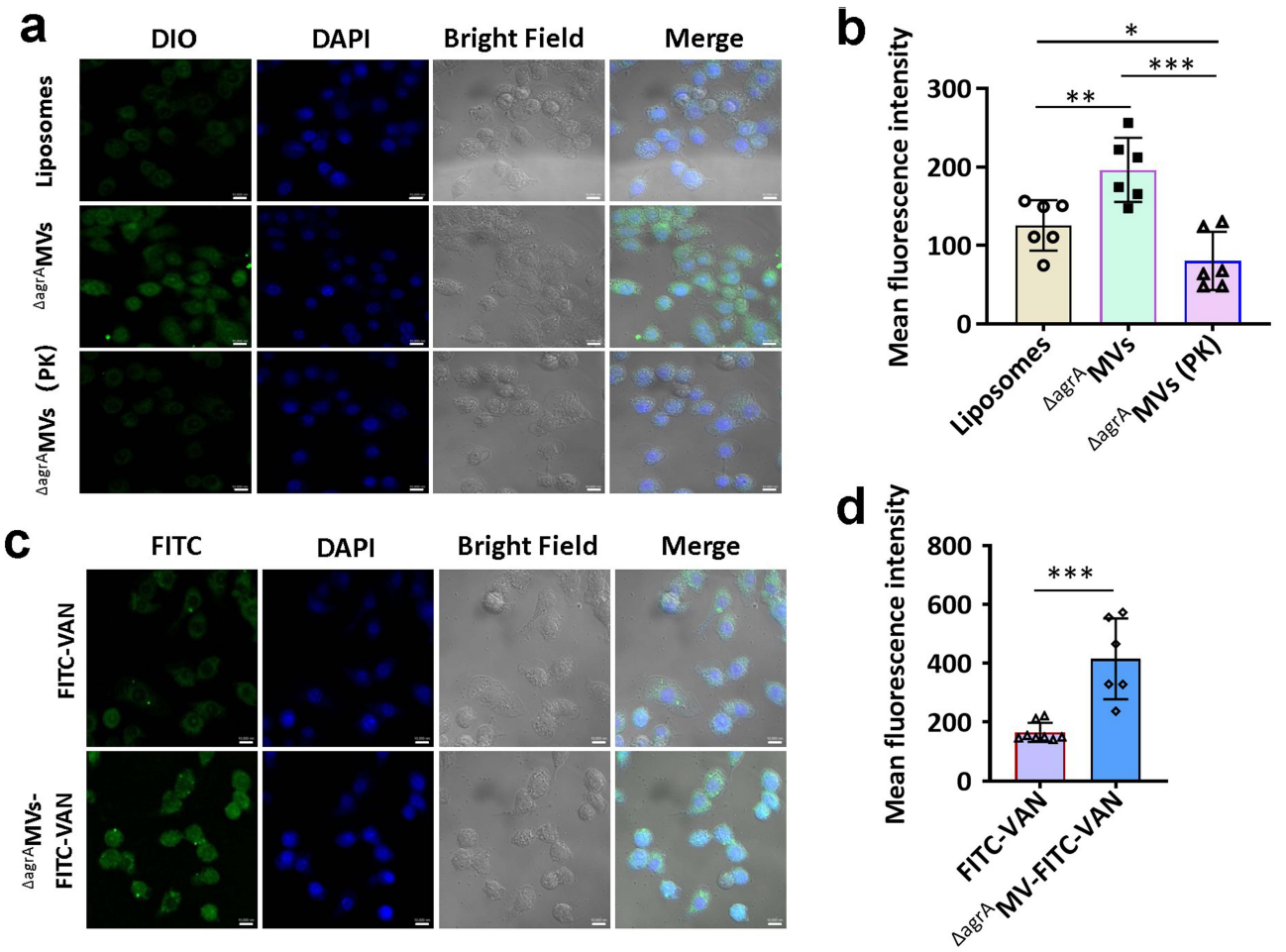

Figure 3 Cellular uptake of $^{\Delta agrA}$MV nanoparticles by macrophages. (**a**) Protease K (PK) pretreatment decreased macrophage internalization of $^{\Delta agr}$AMVs. Liposomes served as negative controls. Green signals within cells represent internalized $^{\Delta agrA}$MVs, and blue ones indicate cell nuclei (40× magnification), Scale bars: 10 μm. (**b**) Quantitative analysis of $^{\Delta agrA}$ MV uptake. Fluorescence intensity was measured in 149 liposome-treated cells, 142 $^{\Delta agrA}$MVs-treated cells, or 122 $^{\Delta agrA}$MVs (PK)-treated cells. (**c**) Enhanced cellular uptake of VAN through $^{\Delta agrA}$MV encapsulation. Scale bars: 10 μm. (**d**) Quantitative analysis of FITC-VAN uptake. Fluorescence intensity was measured in 173 FITC-VAN-treated cells or 190 $^{\Delta agrA}$MV-FITC-VAN-treated cells. Data are shown as mean ± SEM. Statistical significance was measured by Student's *t*-test, **P* < 0.05, ***P* < 0.01, and *** *P*< 0.001.

PBS, VAN, and liposome groups, which displayed similar cytokine profiles. The increased TNF-α and IL-6 levels suggest M1 polarization of macrophages, a phenotype associated with enhanced bacterial clearance.[38,44]

CD86, a hallmark of M1 macrophages,[2] was analyzed by flow cytometry. Treatment with *S. aureus* $^{\Delta agrA}$MVs for 12 or 24 h substantially increased the proportion of $CD86^+$ macrophages compared to the untreated and PBS control groups (Figure 4c and d), further supporting M1 polarization of RAW264.7 cells. This finding was further confirmed by immunofluorescence staining (Figure 4e and f). Collectively, these results demonstrate that *S. aureus* RN4220Δ*agrA*-derived $^{\Delta agrA}$MVs induce M1 macrophage polarization, thereby facilitating intracellular bacterial clearance.

Effect of $^{\Delta agrA}$MVs on MRSA Killing by Macrophages

Since M1 macrophages promote pathogen clearance,[2,38] we investigated the effect of $^{\Delta agrA}$MVs on macrophage antibacterial activity. RAW264.7 macrophages were infected with MRSA USA300 at an MOI of 15. After 2 h of infection, cells were treated with PBS, VAN, liposomes, or $^{\Delta agrA}$MVs for 12 h. Plate counting revealed a remarkable reduction in intracellular MRSA load in macrophages treated with $^{\Delta agrA}$MVs compared to the PBS control (Figure 5a). Although VAN treatment also considerably reduced MRSA burden in macrophages, liposomes did not contribute to MRSA killing by macrophages. These data indicate that $^{\Delta agrA}$MVs promote macrophage-mediated clearance of intracellular MRSA.

https://doi.org/10.2147/IJN.S524445

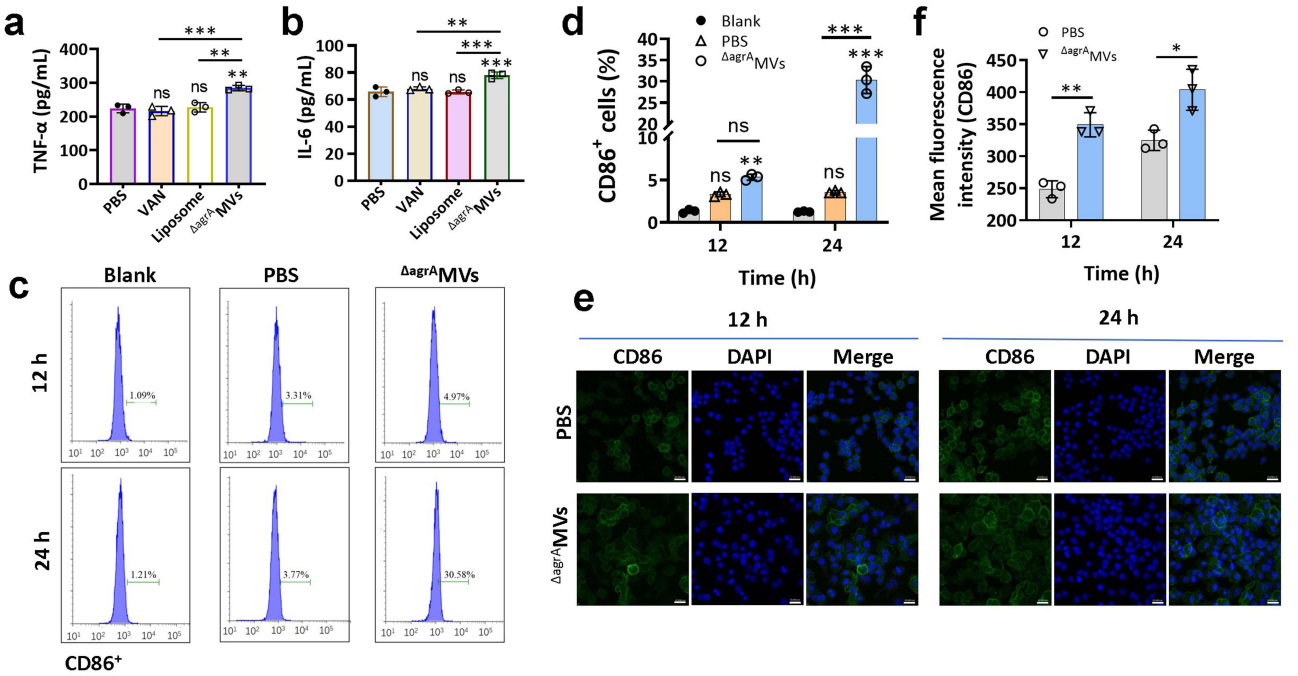

Figure 4 Effect of $^{\Delta agrA}$MVs on macrophages polarization. (**a** and **b**) Cytokine levels of (**a**) TNF-α and (**b**) IL-6 secreted from RAW264.7 macrophages after 12 h treatment with PBS, VAN, Liposome, and $^{\Delta agrA}$MVs. (**c** and **d**) Flow cytometric analysis of M1 polarization: (**c**) Representative flow cytometry plots of CD86$^+$ macrophages, (**d**) Quantification of CD86$^+$ cell populations post-treatment. (**e** and **f**) Immunofluorescence analysis: (**e**) CLSM images of CD86$^+$ macrophages (red: CD86, blue: DAPI; Scale bars: 10 μm), and (**f**) Quantitative fluorescence intensity of CD86 staining. All experiments were performed in triplicate. Data are shown as mean ± SD (cytokine/flow data) or SEM (fluorescence intensity). The difference was analyzed by one-way or two-way ANOVA. *P < 0.05, **P < 0.01, *** P< 0.001, and ns represents no significance.

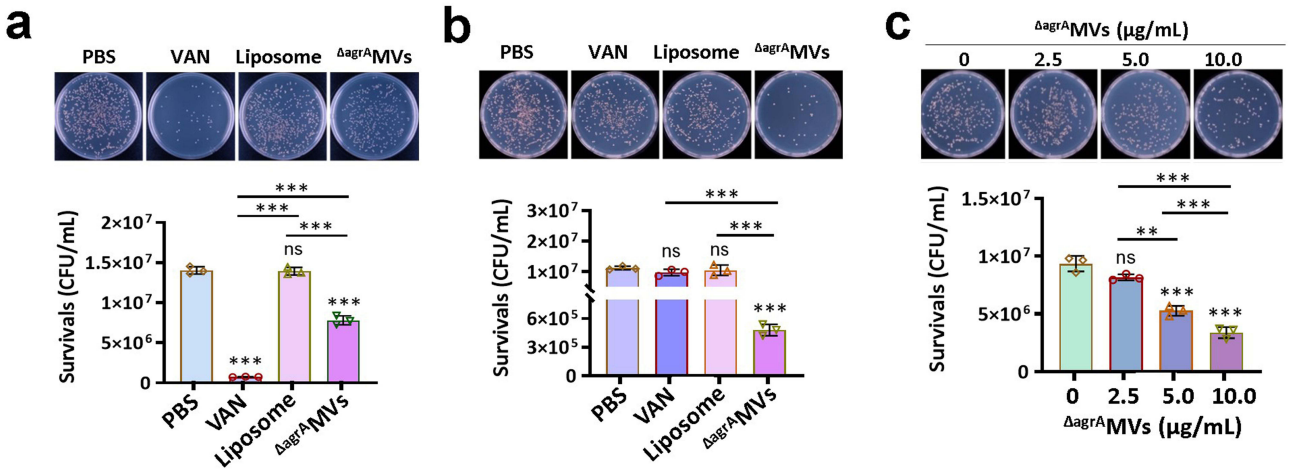

Figure 5 Enhancement of MRSA clearance in macrophages by $^{\Delta agrA}$MVs. (**a**) Promotion of macrophage intracellular bacterial clearance by $^{\Delta agrA}$MVs. RAW264.7 cells were infected with MRSA USA300 at an MOI of 15, followed by treatment with PBS, VAN, liposomes, or $^{\Delta agrA}$MVs after 2 h post-infection. Representative images of surviving bacterial colonies on BHI agar plates after 12 h of treatment (up panel), and quantitative analysis of bacterial counts (bottom panel). (**b**) Protective effect against MRSA infection. RAW264.7 cells were pretreated for 2 h with PBS, VAN, liposomes, or $^{\Delta agrA}$MVs, and then infected with USA300. Intracellular MRSA load was counted by plate assay after 12 h infection. (**c**) Dose-dependent protection by $^{\Delta agrA}$MVs. RAW264.7 cells were pretreated for 2 h with various concentrations of $^{\Delta agrA}$MVs before MRSA infection. Bacterial counts measured after 12 h infection. All experiments were repeated three times. Data are shown as mean ± SD. Statistical significance was calculated by one-ANOVA, **P < 0.01, *** P< 0.001, and ns represents no significance.

Next, we determined whether $^{\Delta agrA}$MVs could prevent MRSA infection in macrophages. RAW264.7 cells were pretreated with PBS, VAN, liposomes, or $^{\Delta agrA}$MVs for 2 h prior to MRSA infection. After 12 h of infection, intracellular bacteria were counted using a plate assay.[45] $^{\Delta agrA}$MV pretreatment significantly decreased intracellular MRSA burden compared to PBS (P < 0.001; Figure 5b), with dose-dependent protection observed (Figure 5c). In contrast, neither VAN nor liposomes

conferred prophylactic effects against MRSA infection (Figure 5b). These results indicate that *S. aureus* $^{\Delta agrA}$MVs protect macrophages from MRSA infection and that $^{\Delta agrA}$MV-activated macrophages efficiently eliminate intracellular MRSA.

Effect of $^{\Delta agrA}$MV-VAN on Intracellular MRSA Killing

Given the macrophage-activating effect of *S. aureus* $^{\Delta agrA}$MVs, we determined whether $^{\Delta agrA}$MV encapsulation enhances the efficacy of VAN against intracellular MRSA in macrophages. RAW264.7 cells were seeded at 1×10^5 cells/well and cultured overnight in 5% CO_2. Cells were then infected with *S. aureus* USA300 at an MOI of 20 for 2 h, followed by treatment with PBS (control), VAN alone, $^{\Delta agrA}$MVs alone, $^{\Delta agrA}$MV+VAN, or $^{\Delta agrA}$MV-VAN for 12 or 24 h. As shown in Figure 6a–c, $^{\Delta agrA}$MV-VAN treatment considerably reduced intracellular MRSA number compared to VAN alone at both time points ($P < 0.01$ or 0.001). While $^{\Delta agrA}$MVs and VAN combination also remarkably decreased intracellular MRSA burden, the $^{\Delta agrA}$MV-VAN group showed the lowest bacterial survival rate (Figure 6b and c), indicating that VAN encapsulation in $^{\Delta agrA}$MVs synergistically promotes bacterial clearance. This effect may be attributed to either $^{\Delta agrA}$MV-induced macrophage activation or improved intracellular VAN delivery via $^{\Delta agrA}$MVs, both of which could augment bactericidal activity against intracellular MRSA.[18,38] Notably, the specific mechanism of MRSA neutralization was not elucidated. A recent study revealed that *E. coli*-derived MVs are preferentially internalized by *E. coli* and other Gram-negative bacteria like *Klebsiella* pneumoniae, but not by Gram-positive bacteria like *S. aureus*,[32] highlighting the homotypic targeting capability of bacterial MVs.[31] We hypothesize that VAN-loaded isogenous MVs may selectively target MRSA-infected macrophages, thereby improving intracellular bacterial clearance. Overall, the $^{\Delta agrA}$MV-VAN formulation showed potent intracellular bactericidal activity against MRSA, indicating significant potential as a therapeutic strategy for MRSA-refractory infections.

In vivo Anti-MRSA Efficacy of $^{\Delta agrA}$MV-VAN

The persistent intracellular presence of *S. aureus* is a major contributor to recurrent infections,[5] primarily due to the limited ability of antibiotics to penetrate host cells.[12] Our results demonstrated that encapsulation of VAN in $^{\Delta agrA}$MVs increased its cellular

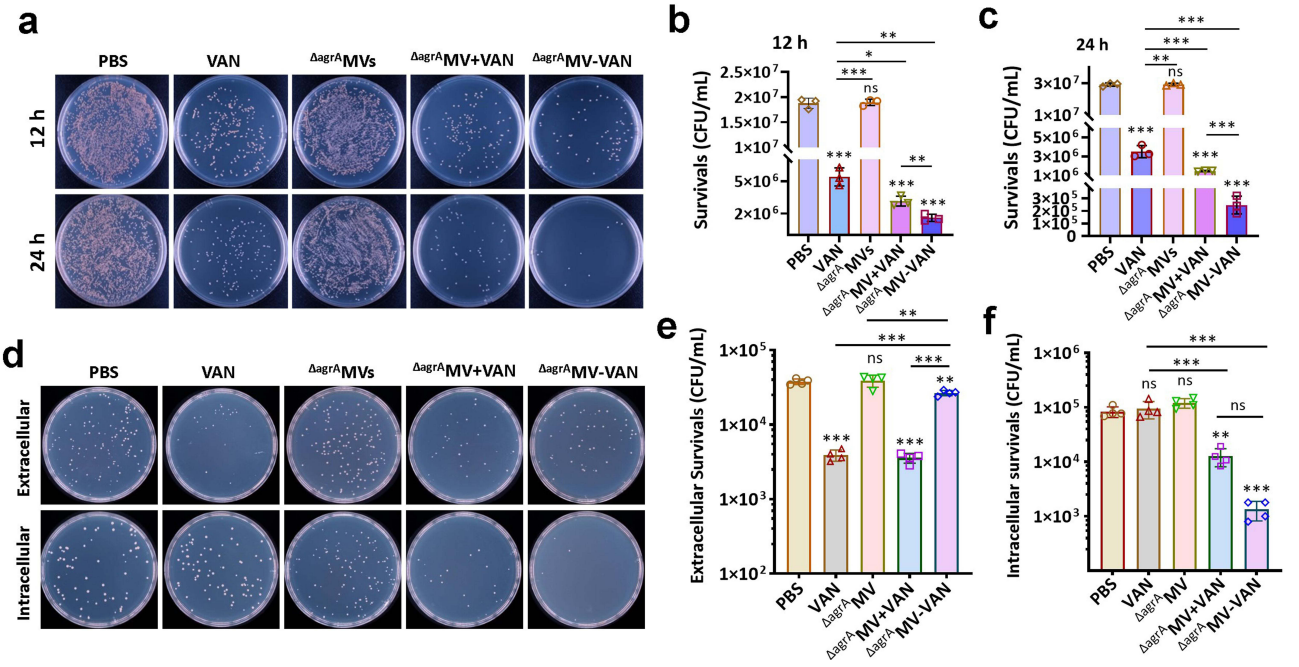

Figure 6 $^{\Delta agrA}$MV-VAN eliminates intracellular MRSA in vitro and in vivo. (**a**) Survival of USA300 on BHI plates. RAW264.7 macrophages were infected with MRSA USA300 (MOI = 20) for 2 h, then treated with PBS, VAN, $^{\Delta agrA}$MVs, $^{\Delta agrA}$MV+VAN, or $^{\Delta agrA}$MV-VAN for 12 or 24 h. Intracellular MRSA was quantified by plate counting at: (**b**) 12 h and (**c**) 24 h post-treatment. (**d**) In vivo bacterial clearance. BALB/c mice (n = 4 per group) were intraperitoneally challenged with 5×10^7 CFU of MRSA USA300, then treated intraperitoneally with PBS, VAN, $^{\Delta agrA}$MVs, $^{\Delta agrA}$MV+VAN, or $^{\Delta agrA}$MV-VAN. Peritoneal fluids were collected after 24 h for quantification of: (**e**) Extracellular and (**f**) Intracellular bacterial loads. Data are shown as mean ± SD. Statistical significance was measured by one-way ANOVA, *$P < 0.05$, **$P < 0.01$, *** $P< 0.001$, and ns represents no significance.

https://doi.org/10.2147/IJN.S524445

internalization (Figure 3c and d) and promoted intracellular MRSA clearance by RAW264.7 macrophages (Figure 6a–c). To evaluate the in vivo antibacterial efficacy of $^{\Delta agrA}$MV- VAN, we established a mouse model of abdominal infection as previously described.[17] Peritoneal fluid samples were collected 24 h post-treatment with PBS, VAN, $^{\Delta agrA}$MVs, $^{\Delta agrA}$MV+VAN, or $^{\Delta agrA}$MV-VAN (n = 4 per group). As shown in Figure 6d, both VAN and $^{\Delta agrA}$MV+VAN treatments substantially reduced extracellular bacterial loads compared to PBS ($P < 0.001$). While $^{\Delta agrA}$MV-VAN also decreased extracellular bacteria ($P < 0.01$), its efficacy was lower than VAN alone or the physical mixture (Figure 6e). Notably, the $^{\Delta agrA}$MV+VAN combination displayed superior intracellular bactericidal effects compared to VAN alone, consistent with in vitro results (Figure 6a–c). Although statistical difference was not reached relative to the combination group, $^{\Delta agrA}$MV-VAN treatment exhibited the lowest intracellular MRSA burden among all groups (Figure 6f). Overall, these data indicate that the $^{\Delta agrA}$MV-VAN formulation efficiently eradicates intracellular MRSA in vivo, highlighting its therapeutic potential for persistent infections.

Safety Assessment

Compared to MVs secreted by the wild-type RN4220 strain, $^{\Delta agrA}$MVs derived from *S. aureus* RN4220Δ*agrA* exhibit lower toxicity.[25] To assess the biocompatibility of $^{\Delta agrA}$MV-VAN, RAW264.7 cells were treated with various concentrations (0, 25, 50,100, and 200 μg/mL) of $^{\Delta agrA}$MV-VAN for different durations (2, 6, 12, and 24 h). Cell viability remained unaffected within the first 12 h of treatment (Figure 7a). Interestingly, a 24 h treatment with $^{\Delta agrA}$MV-VAN remarkably increased cell proliferation compared to untreated controls. This effect may be attributed to uncertain proliferative molecules involved in $^{\Delta agrA}$MV nanoparticles, though the precise mechanism warrants further investigation.

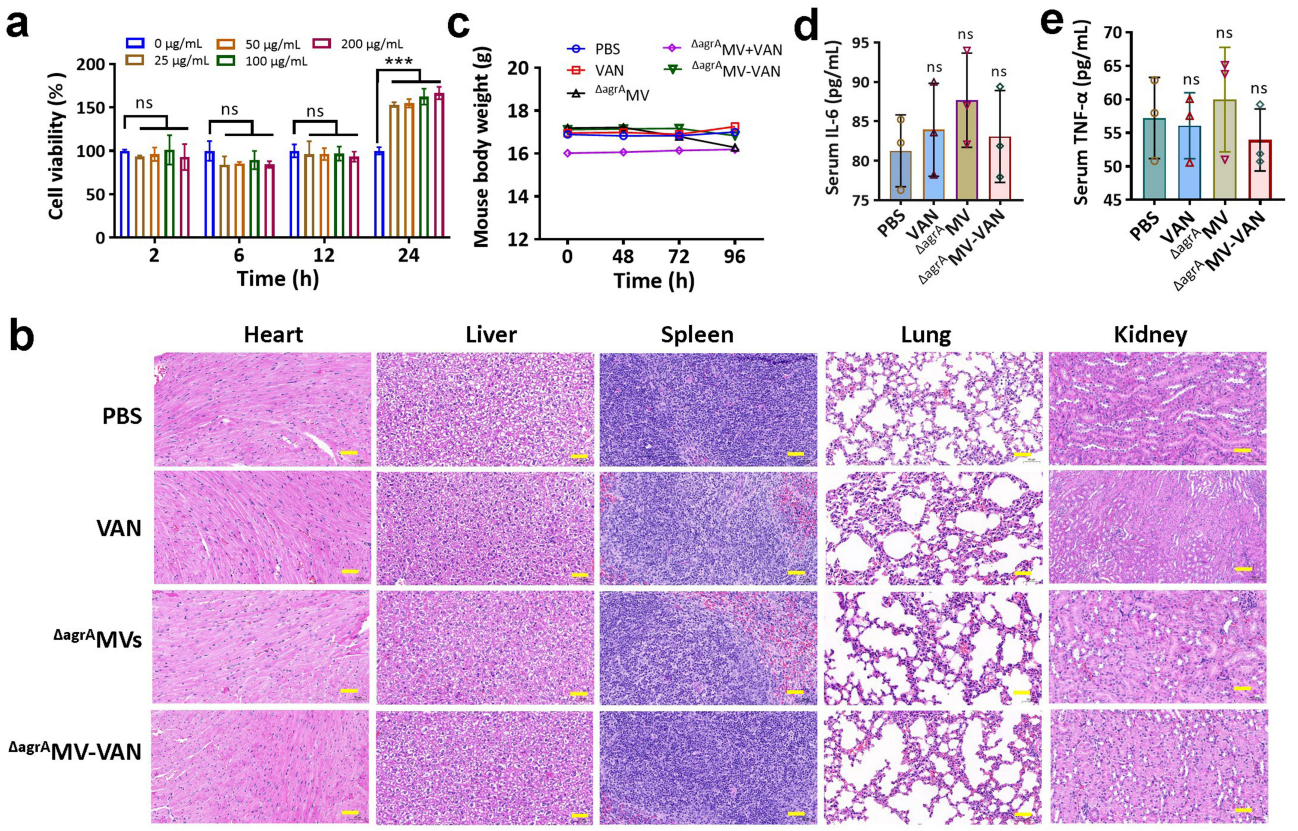

Figure 7 Safety assessment of $^{\Delta agrA}$MV-VAN. (**a**) Toxic effects of $^{\Delta agrA}$MV-VAN on RAW264.7 macrophages. RAW264.7 cells were treated with diverse concentrations (0, 25, 50, 100, and 200 μg/mL) of $^{\Delta agrA}$MV-VAN for the indicated time periods. Cell viability was detected using a Cell Counting Kit. The viability of untreated cells (0 μg/mL) was set as 100%, and the relative viability of other groups was calculated and shown. (**b**) H&E staining of mouse organ sections. Organs from BALB/c mice challenged with PBS, VAN, $^{\Delta agrA}$MVs, and $^{\Delta agrA}$MV-VAN were collected, sectioned, and subjected to H&E staining. Scale bars: 50 μm. (**c**) Changes in mouse body weight. (**d**) Blood IL-6 levels in mice 6 h post-challenge. (**e**) Blood TNF-α levels. Data are shown as mean ± SD. Statistical significance was measured by one-way or two-way ANOVA; *** P<0.001, and ns indicates no significance.

We next investigated the in vivo toxicity of $^{\Delta agrA}$MV-VAN in a murine infection model. BALB/c mice were intraperitoneally injected with PBS, VAN, $^{\Delta agrA}$MVs, or $^{\Delta agrA}$MV-VAN. After 24 h post-injection, mouse organs (heart, liver, spleen, lungs, and kidneys) were harvested and sectioned for analysis. H&E staining revealed normal histomorphology in all all treatment groups, with no pathological alterations observed (Figure 7b). Additionally, $^{\Delta agrA}$MV-VAN treatment did not affect body weight or systemic levels of IL-6 and TNF-α compared to controls (Figure 7c–e). Collectively, these findings demonstrate that the $^{\Delta agrA}$MV-VAN formulation is biocompatible in vitro and non-toxic in vivo, supporting its potential as a safe and effective therapeutic for persistent MRSA infections.

Conclusion

We developed $^{\Delta agrA}$MV-VAN to achieve intracellular uptake and accumulation of therapeutic agents by MRSA-infected macrophages, enabling sustained elimination of intracellular MRSA. However, this study has several limitations. First, although multiple mass ratios (1:1, 1:2, and 2:1) were determined, the VAN loading efficiency in $^{\Delta agrA}$MV-VAN remained limited (21.6%). Novel preparation methods, such as using hybrid cellular MVs,[27,46] may improve VAN loading capacity and warrant further exploration. Second, while MRSA can infect virtually all human organs, the tissue-targeting capability of $^{\Delta agrA}$MV-VAN was not evaluated. Additional infectious models, such as endocarditis and meningitis, are needed to conduct the therapeutic efficacy of $^{\Delta agrA}$MV-VAN in diverse pathological contexts. Third, although bacterial MVs contain certain PAMPs that may modulate macrophage activation,[41–43] the specific PAMPs in $^{\Delta agrA}$MVs responsible for M1 macrophage polarization remain unidentified. Future studies employing proteomic analysis and genetic screening could elucidate the mechanistic basis of $^{\Delta agrA}$MVs-mediated macrophage activation. In summary, this study provides a promising strategy against intracellular MDR infections and offers a rational framework for designing exogenous antibacterial nanomaterials.

Data Sharing Statement

Additional information is available from the correspondence author based on reasonable request.

Ethics Approval

All animal experiments were performed in accordance with the Regulations for the Administration of Affairs Concerning Experimental Animals approved by the State Council of the People's Republic of China, and animal procedures were reviewed and approved by the Animal Use and Care Administrative Advisory Committee of the Army Medical University (protocol no. AMUWEC2020735).

Acknowledgments

This study was supported by the National Natural Science Foundation of China (82071857 and 82272341).

Disclosure

The authors declare no conflicts of interest in this work.

References

1. Murray CJL, Ikuta KS, Sharara F, et al. Global burden of bacterial antimicrobial resistance in 2019: a systematic analysis. *Lancet*. 2022;399 (10325):629–655. doi:10.1016/S0140-6736(21)02724-0
2. Abebe AA, Birhanu AG. Methicillin resistant *Staphylococcus aureus*: molecular mechanisms underlying drug resistance development and novel strategies to combat. *Infect Drug Resist*. 2023;16:7641–7662. doi:10.2147/IDR.S428103
3. Yu YJ, Yan JH, Chen QW, et al. Polymeric nano-system for macrophage reprogramming and intracellular MRSA eradication. *J Control Release*. 2023;353:591–610. doi:10.1016/j.jconrel.2022.12.014
4. Dhankhar P, Dalal V, Kotra DG, Kumar P. *In-silico* approach to identify novel potent inhibitors against GraR of *S. aureus*. *Front Biosci*. 2020;25 (7):1337–1360. doi:10.2741/4859
5. Dalal V, Dhankhar P, Singh V, et al. Structure-based identification of potential drugs against FmtA of *Staphylococcus aureus*: virtual screening, molecular dynamics, MM-GBSA, and QM/MM. *Protein J*. 2021;40(2):148–165. doi:10.1007/s10930-020-09953-6
6. Kumari R, Rathi R, Pathak SR, Dalal V. Structural-based virtual screening and identification of novel potent antimicrobial compounds against YsxC of *Staphylococcus aureus*. *J Mol Struct*. 2022;1255:132476. doi:10.1016/j.molstruc.2022.132476

7. Kumari R, Dalal V. Identification of potential inhibitors for LLM of *Staphylococcus aureus*: structure-based pharmacophore modeling, molecular dynamics, and binding free energy studies. *J Biomol Struct Dyn*. 2022;40(20):9833–9847. doi:10.1080/07391102.2021.1936179
8. Turner NA, Sharma-Kuinkel BK, Maskarinec SA, et al. Methicillin-resistant *Staphylococcus aureus*: an overview of basic and clinical research. *Nat Rev Microbiol*. 2019;17(4):203–218. doi:10.1038/s41579-018-0147-4
9. Jorch SK, Surewaard BG, Hossain M, et al. Peritoneal GATA6+ macrophages function as a portal for *Staphylococcus aureus* dissemination. *J Clin Invest*. 2019;129(11):4643–4656. doi:10.1172/JCI127286
10. Rao Y, Peng H, Shang W, et al. A vancomycin resistance-associated WalK(S221P) mutation attenuates the virulence of vancomycin-intermediate *Staphylococcus aureus*. *J Adv Res*. 2022;40:167–178. doi:10.1016/j.jare.2021.11.015
11. al-Nawas B, Shah PM. Intracellular activity of vancomycin and Ly333328, a new semisynthetic glycopeptide, against methicillin-resistant *Staphylococcus aureus*. *Infection*. 1998;26(3):165–167. doi:10.1007/BF02771843
12. Xie S, Tao Y, Pan Y, et al. Biodegradable nanoparticles for intracellular delivery of antimicrobial agents. *J Control Release*. 2014;187:101–117. doi:10.1016/j.jconrel.2014.05.034
13. Herrmann IK, Wood MJA, Fuhrmann G. Extracellular vesicles as a next-generation drug delivery platform. *Nat Nanotechnol*. 2021;16(7):748–759. doi:10.1038/s41565-021-00931-2
14. Zhou K, Li C, Chen D, et al. A review on nanosystems as an effective approach against infections of *Staphylococcus aureus*. *Int J Nanomed*. 2018;13:7333–7347. doi:10.2147/IJN.S169935
15. Hulme J. Application of nanomaterials in the prevention, detection, and treatment of methicillin-resistant *Staphylococcus aureus* (MRSA). *Pharmaceutics*. 2022;14(4):805. doi:10.3390/pharmaceutics14040805
16. Lin X, He J, Li W, et al. Lung-targeting lysostaphin microspheres for methicillin-resistant *Staphylococcus aureus* pneumonia treatment and prevention. *ACS Nano*. 2021;15(10):16625–16641. doi:10.1021/acsnano.1c06460
17. Yang X, Xie B, Peng H, et al. Eradicating intracellular MRSA via targeted delivery of lysostaphin and vancomycin with mannose-modified exosomes. *J Control Release*. 2021;329:454–467. doi:10.1016/j.jconrel.2020.11.045
18. Xie B, Zhao H, Zhang R, et al. Bacteria-mimetic nanomedicine for targeted eradication of intracellular MRSA. *J Control Release*. 2023;357:371–378. doi:10.1016/j.jconrel.2023.03.053
19. Jahromi LP, Fuhrmann G. Bacterial extracellular vesicles: understanding biology promotes applications as nanopharmaceuticals. *Adv Drug Deliv Rev*. 2021;173:125–140. doi:10.1016/j.addr.2021.03.012
20. Yuan J, Yang J, Hu Z, et al. Safe staphylococcal platform for the development of multivalent nanoscale vesicles against viral infections. *Nano Lett*. 2018;18(2):725–733. doi:10.1021/acs.nanolett.7b03893
21. Wang X, Eagen WJ, Lee JC. Orchestration of human macrophage NLRP3 inflammasome activation by *Staphylococcus aureus* extracellular vesicles. *Proc Natl Acad Sci U S A*. 2020;117(6):3174–3184. doi:10.1073/pnas.1915829117
22. Ding C, He R, Cheng T, et al. Bacterial outer membrane-based biomimetic immune adaptors: mild immunomodulatory and bacterial targeted delivery strategy against implant-related infections. *Adv Funct Mater*. 2023;33(42):2304168. doi:10.1002/adfm.202304168
23. Peng X, Chen J, Gan Y, et al. Biofunctional lipid nanoparticles for precision treatment and prophylaxis of bacterial infections. *Sci Adv*. 2024;10(14):eadk9754. doi:10.1126/sciadv.adk9754
24. Wu S, Huang Y, Yan J, et al. Bacterial outer membrane-coated mesoporous silica nanoparticles for targeted delivery of antibiotic rifampicin against Gram-negative bacterial infection in vivo. *Adv Funct Mater*. 2021;31(35):2103442. doi:10.1002/adfm.202103442
25. Chen J, Lv Y, Shang W, et al. Loaded delta-hemolysin shapes the properties of *Staphylococcus aureus* membrane vesicles. *Front Microbiol*. 2023;14:1254367. doi:10.3389/fmicb.2023.1254367
26. Yang X, Shi G, Guo J, Wang C, He Y. Exosome-encapsulated antibiotic against intracellular infections of methicillin-resistant *Staphylococcus aureus*. *Int J Nanomed*. 2018;13:8095–8104. doi:10.2147/IJN.S179380
27. Huang R, Cai GQ, Li J, et al. Platelet membrane-camouflaged silver metal-organic framework drug system against infections caused by methicillin-resistant *Staphylococcus aureus*. *J Nanobiotechnology*. 2021;19(1):229. doi:10.1186/s12951-021-00978-2
28. Yunna C, Mengru H, Lei W, Weidong C. Macrophage M1/M2 polarization. *Eur J Pharmacol*. 2020;877:173090. doi:10.1016/j.ejphar.2020.173090
29. Benoit M, Desnues B, Mege JL. Macrophage polarization in bacterial infections. *J Immunol*. 2008;181(6):3733–3739. doi:10.4049/jimmunol.181.6.3733
30. Lehar SM, Pillow T, Xu M, et al. Novel antibody-antibiotic conjugate eliminates intracellular *S. aureus*. *Nature*. 2015;527(7578):323–328. doi:10.1038/nature16057
31. Podkowik M, Perault AI, Putzel G, et al. Quorum-sensing *agr* system of *Staphylococcus aureus* primes gene expression for protection from lethal oxidative stress. *Elife*. 2024;12:RP89098. doi:10.7554/eLife.89098
32. Jacob KM, Hernández-Villamizar S, Hammer ND, Reguera G. Mucin-induced surface dispersal of *Staphylococcus aureus* and *Staphylococcus epidermidis* via quorum-sensing dependent and independent mechanisms. *mBio*. 2024;15(8):e0156224. doi:10.1128/mbio.01562-24
33. Haney MJ, Klyachko NL, Zhao Y, et al. Exosomes as drug delivery vehicles for Parkinson's disease therapy. *J Control Release*. 2015;207:18–30. doi:10.1016/j.jconrel.2015.03.033
34. Moldovan A, Wagner F, Schumacher F, et al. Chlamydia trachomatis exploits sphingolipid metabolic pathways during infection of phagocytes. *mBio*. 2025;18(5):e0398124. doi:10.1128/mbio.03981-24
35. Wang ZJ, Zhu YY, Bai L-Y. Bai LY, et al.A new therapeutic strategy for infectious diseases against intracellular multidrug-resistant bacteria. *J Control Release*. 2024;375:467–477. doi:10.1016/j.jconrel.2024.09.028
36. Yang X, Shi G, Lin Z, et al. Pathogen-targeting biomineralized bacterial outer membrane vesicles for eradicating both intracellular and extracellular *Staphylococcus aureus*. *J Control Release*. 2025;382:113702. doi:10.1016/j.jconrel.2025.113702
37. Turner AB, Giraldo-Osorno PM, Douest Y, et al. Race for the surface between THP-1 macrophages and *Staphylococcus aureus* on various titanium implants with well-defined topography and wettability. *Acta Biomater*. 2025;191:113–139. doi:10.1016/j.actbio.2024.11.013
38. Mège JL, Mehraj V, Capo C. Macrophage polarization and bacterial infections. *Curr Opin Infect Dis*. 2011;24(3):230. doi:10.1097/QCO.0b013e328344b73e
39. Eisele NA, Ruby T, Jacobson A, et al. Salmonella require the fatty acid regulator PPARdelta for the establishment of a metabolic environment essential for long-term persistence. *Cell Host Microbe*. 2013;14(2):171–182. doi:10.1016/j.chom.2013.07.010

40. Lee AR, Park SB, Kim SW, et al. Membrane vesicles from antibiotic-resistant *Staphylococcus aureus* transfer antibiotic-resistance to antibiotic-susceptible *Escherichia coli*. *J Appl Microbiol*. 2022;132(4):2746–2759. doi:10.1111/jam.15449
41. Kaparakis-Liaskos M, Ferrero RL. Immune modulation by bacterial outer membrane vesicles. *Nat Rev Immunol*. 2015;15(6):375–387. doi:10.1038/nri3837
42. Mehanny M, Koch M, Lehr CM, Fuhrmann G. Streptococcal extracellular membrane vesicles are rapidly internalized by immune cells and alter their cytokine release. *Front Immunol*. 2020;11:80. doi:10.3389/fimmu.2020.00080
43. Bitto NJ, Cheng L, Johnston EL, et al. *Staphylococcus aureus* membrane vesicles contain immunostimulatory DNA, RNA and peptidoglycan that activate innate immune receptors and induce autophagy. *J Extracell Vesicles*. 2021;10(6):e12080. doi:10.1002/jev2.12080
44. Kadomoto S, Izumi K, Mizokami A. Macrophage polarity and disease control. *Int J Mol Sci*. 2021;23(1):144. doi:10.3390/ijms23010144
45. Liu H, Wei X, Wang Z, et al. LysSYL: a broad-spectrum phage endolysin targeting *Staphylococcus species* and eradicating *S. aureus* biofilms. *Microb Cell Fact*. 2024;23(1):89. doi:10.1186/s12934-024-02359-4
46. Zhang S, Chen T, Lu W, et al. Hybrid cell membrane-engineered nanocarrier for triple-action strategy to address *Pseudomonas aeruginosa* infection. *Adv Sci*. 2025;12(6):e2411261. doi:10.1002/advs.202411261